Loosely - coupled numerical simulation of Helicopter Aeromechanics using an unstructured CFD solver

F. Bensing* and M. Keßler† and E. Krämer‡
Institut für Aerodynamik und Gasdynamik, University of Stuttgart, Germany

Abstract

Problems in helicopter interactional aerodynamics, in particular tail shake and pitch up phenomena, require very detailed geometrical modelling in the inner rotor area. As mesh generation becomes more and more excessive in terms of time consumption for structured-type grids, the only feasible alternative is the transition to an unstructured simulation environment.
In this work an extension of the unstructured TAU flow solver (DLR) is presented which allows for weak fluid-structure coupling on the main rotor blades. The new toolchain is validated against and compared to the standard structured tool involving the flow solver FLOWer (DLR) in the context of an isolated rotor test case in wind tunnel conditions, corresponding to the low-speed pitch up case of the GOAHEAD experiment. Good agreement between the two respective toolchains is achieved and good performance of the new simulation environment in terms of scalability and peak performance is measured on a NEC Nehalem massively-parallel cluster platform.

Abbreviations

ALE	Arbitrary Lagrangian Eulerian
CAD	Computer Aided Design
CFD	Computational Fluid Dynamics
CSD	Computational Structural Dynamics
DLR	Deutsches Zentrum für Luft- und Raumfahrt
DNW	Deutsch-Niederländischer Windkanal
FLOPS	Floating Point Operations Per Second
GCL	Geometric Conservation Law
GOAHEAD	Generation of Advanced Helicopter Experimental Aerodynamic Database
HART	HHC Aeroacoustics Rotor Test
HHC	Higher Harmonic Control
HLRS	High Performance Computing Center Stuttgart
HOST	Helicopter Overall Simulation Tool
IAG	Institut für Aerodynamik und Gasdynamik
LSPU	Low Speed Pitch Up
MPI	Message Passing Interface
URANS	Unsteady Reynolds-averaged Navier Stokes

I. Introduction

Part of the research at the Institut für Aerodynamik und Gasdynamik at the University of Stuttgart has been strongly focused on helicopter main rotor aerodynamics and aeroelasticity in the past years. Within this context fluid-structure coupling at the main rotor blades has proven mandatory for a realistic representation of the flow physics, particularly in forward flight. Coupling can be performed in several ways: either data exchange between the flow and structural solver is done on a time step basis (strong coupling) or on a per-period basis (weak coupling). Strong coupling, which due to its time-accurate procedure can be applied to any flight case, has been a field of extensive research at IAG in the past [1, 2, 3]. However, many flight scenarios such as constant speed forward or stationary curved flight involve

periodic conditions. In this case, weak coupling enforcing this periodicity is likely to allow for a much faster convergence. Consequently, weak coupling at isolated main rotors has also been applied at IAG in those flight conditions [4].
Besides the aeroelastic coupling at the main rotor blades, some sort of trim procedure has to be employed in order to ensure that a specified flight dynamic state of the rotor is reached. In this sense, a rotor trim is defined by the action of numerically reproducing certain rotor parameters of a corresponding experiment.
Beginning with simulations of isolated rotors, research steered towards the simulation of complete helicopter configurations [5, 6]. To date, all simulations were conducted following a structured grid approach. As part of the current activities at IAG, helicopter main rotor-fuselage interactional phenomena such as the well known tail shake effect, which are still encountered during flight testing of many helicopter prototypes [7, 8, 9] are to be investigated. Such investigations call for a substantial enrichment in geometrical detail, especially in the inner hub region of the main rotor. Here, the structured grid generation process suffers from excessive manual time consumption and eventually becomes impossible. Therefore, efforts at IAG are currently made to build up a new toolchain around the DLR unstructured flow solver TAU. Within these activities, the weak coupling methodology has been extended to unstructured grids of arbitrarily mixed element types. Results for an isolated rotor setup in low speed pitch up conditions corresponding to the GOAHEAD experiment were obtained using our standard structured (FLOWer) and new unstructured (TAU) toolchains. In both cases, structural dynamics and the trim of the rotor was done employing the flight mechanics code HOST by Eurocopter [10].

II. Numerical Methodology

A. Computational Fluid Dynamics

Two CFD codes for the solution of the three-dimensional, unsteady Reynolds-averaged Navier-Stokes (URANS) equations were compared in this work. Our standard toolchain makes use of the FLOWer code (DLR) [11, 12]. This simulation environment has been in wide use for the simulation of weakly-coupled helicopter rotor configurations for several years now and is taken as a reference for validation of our new toolchain built around the TAU code. The FLOWer code is based on a finite volume formulation on block-structured grids. Central and upwind spatial discretisations are implemented. In the present work, the central scheme of formally second order accuracy on smooth meshes is applied using a cell-centered metric. Artificial dissipation using a blend of second and forth order difference operators according to Jameson [13] is incorporated for damping of high frequency oscillations.
TAU features a finite volume discretisation on unstructured grids of mixed element type. As for FLOWer, a central space discretisation with artificial dissipation is employed. In both codes, time integration is done via dual time-stepping according to Jameson [14], transforming each of the unsteady physical time steps to the solution of a steady-state solution in pseudo-time. Runge-Kutta integration is applied for pseudo-time marching in a similar manner as for steady-state problems enabling various convergence acceleration techniques. Arbitrary mesh cell movement is enabled following an Arbitrary Lagrangian Eulerian (ALE) approach, incorporating additional fluxes due to cell movement and/or deformation. Accuracy and stability are enhanced by the satisfaction of a discrete Geometric Conservation Law (GCL) [15]. The use of the Chimera technique of overlapping grids renders possible large relative grid movements such as main rotor blade rotation.

B. Computational Structural Dynamics

Fluid-structure coupling between the two respective CFD codes was done using the Eurocopter flight mechanics software HOST, a general purpose computational environment for the simulation and stability analysis of complete helicopters involving all their substructures, as well as isolated rotors. HOST is also capable of trimming a rotor towards prescribed objectives based

on lifting line methodology and two-dimensional airfoil tables. Various semi-empirical models to improve HOST's internal aerodynamics are available such as analytical induced velocity distributions or couplings to prescribed or free wake models. In case of CFD-CSD coupling the HOST-internal representation of the aerodynamics is only of little relevance since these variables are to be replaced by CFD aerodynamic data during the weak coupling process. The elastic blade model inside HOST consists of a quasi one-dimensional Euler-Bernoulli beam where deflections in flap and lag directions as well as elastic torsion along the blade axis are permitted. Simplifications are made in terms of a linear material law and neglection of shear deformation as well as tension elongation. Possible mismatches of the local cross-sectional centers of gravity, tension and shear are taken into account, which allow for couplings between bending and torsional degrees of freedom. The blade is modelled as a sequence of rigid elements, which are connected by virtual joints, permitting geometrical nonlinearity. At each joint, rotations about the lag, flap and torsional axes are allowed. The resulting large number of degrees of freedom is then reduced employing a modal Rayleigh-Ritz approach such that the deformation is finally described by a sum of a limited set of mode-like deformation shapes. Thus, any degree of freedom can be expressed as a weighted sum of an azimuth dependent generalised coordinate q_i and a radius dependent modal shape $\hat{h}_i$ as follows:

$$h(r,\psi) = \sum_{i=1}^{n} q_i(\psi) \cdot \hat{h}_i(r) \quad ,$$

where the sum is taken over all n modes considered.

C. Weak Coupling Methodology and Trim Procedure

As already stated above, weak coupling involves data exchange between CFD and CSD on a periodical basis, i.e. for an n-bladed rotor n/rev periodicity of the flow solution is first to be established before passing the aerodynamic data to the CSD solver. While in transfer from CFD to CSD, these data consist of blade-sectional forces and moments, and corresponding deformations are transferred back from CSD to CFD.
Concurrently, an update of the rotor control angles is done in order to reach prescribed trim objectives. In simulations of wind tunnel experiments, three control parameters of the helicopter are set free, namely main rotor collective θ_0 and the two cyclic pitches θ_c and θ_s. For a trim calculation, an equal number of trim objectives has then to be specified. Most commonly, these trim objectives are global time-averaged rotor thrust, pitching and rolling moments as in the HART and HART-II test campaigns [16]. In this study, however, a pure force trim was employed, setting the three components of the integral averaged rotor forces as trim objectives. Within the context of this work, the trim procedure is restricted to wind tunnel trim conditions at isolated rotors. Aerodynamic loads on other components than the main rotor are not taken into account yet. However, in most experimental cases, also only the main rotor and not the complete helicopter is trimmed towards a specified state.
The fundamental idea of the weak coupling procedure is as follows: three-dimensional CFD loads are used by HOST to correct its internal two-dimensional aerodynamics. Applying this correction, HOST re-trims the rotor. The corresponding blade dynamic response is then taken into account in the subsequent CFD calculation, which yields an update of the aerodynamic loads. Iterative application of this cycle, until the CFD loads match the blade dynamics returned from the HOST trim, ensures that the two-dimensional HOST internal aerodynamics is completely replaced with first principles CFD blade force data. Thus, the coupling procedures involves the following steps:

1. HOST computes an initial rotor trim based on its internal 2D aerodynamics derived from airfoil tables. The complete blade dynamic response is fully described by the modal base and the respective generalized coordinates.

2. A CFD computation is carried out taking into account the blade dynamic response by the reconstruction of the azimuth dependent blade deformation from the modal base and

the respective grid deformation of the blade grids.

3. From the CFD calculation the radial 3D blade load distributions in the rotating hub rotor system (F_x, F_y, F_z in $[N/m]$, M_x, M_y, M_z in $[Nm/m]$) are derived for each azimuth angle and radial station of the blade.

4. In the next trim HOST uses a load given by

$$F^n_{HOST} = F^n_{2D} + F^{n-1}_{3D} - F^{n-1}_{2D},$$

where F^n_{2D} represents the free parameter for the actual HOST trim. A new dynamic blade response is obtained, which is expressed by an update of the generalised coordinates.

5. Steps (2) to (4) are repeated until convergence has been reached, i.e. when the difference

$$\Delta F^n = F^n_{2D} - F^{n-1}_{2D} \to 0\,.$$

Then trim loads depend solely on the three-dimensional CFD aerodynamics and no longer on HOST-internal two-dimensional airfoil data.

The available weak coupling algorithm for structured meshes has in the course of this work been augmented to accomodate unstructured meshes of arbitrary cell types. Hereby the unstructured surface mesh is mapped to a structured-type mesh by means of slicing of the surface cells at radial stations, for which output of the coupling loads that are requested, are specified via input file. In a preprocessing step prior to the unsteady CFD computation, grid point data for each of these radial stations are extracted from the undeformed mesh. These data are then used to reconstruct relevant grid points in deformed state during the unsteady computation as well as for the construction of deformed moment reference points and vectors defining sectional tangents and normals of the blade profiles in a post-processing step. During the integration of the loads for HOST, the algorithm slices the unstructured surface mesh cells according to the possibly flapped and lagged planes corresponding to the respective radii. Subsequently, all cells emerging from this slicing process are subtriangulated and force integration is performed over all these subtriangles. Consequently, triangular as well as quadrilateral blade surface cells can be treated in a generalised manner. Furthermore, only certain so-called aerodynamic parts of the blade surface can be selected to be accounted for loads integration by simple flagging with the help of surface marker information contained in the mesh. This will provide the flexibility to simulate entire and detailed rotors if the user decides that the rotor hub region is of little interest for the pure blade force coupling. Also, fast-prototyped blade grids for testing purposes containing triangular cells on the surface are rendered possible following this approach.

III. Results

A. Experimental Setup

A test case from the GOAHEAD test campaign [17] was selected as a reference in the present study. Experiments were carried out on a fully equipped $1:3.9$ – scaled helicopter configuration mounted in the $6\,\mathrm{x}\,8\,m$ open test section of the German-Dutch wind tunnel (DNW). In the simulations an isolated four-bladed rotor was considered in low speed pitch up conditions featuring a flight Mach number of $Ma = 0.059$, a blade tip Mach number of $Ma_{tip} = 0.617$ and a corresponding rotatory speed of $\Omega = 954\,min^{-1}$, resulting in an advance ratio of $\mu = 0.0956$. This flight case was chosen due to the expectedly slow convergence in the trim iteration process. Geometrically, the blade consists of a rectangular planform of chord length $c = 0.14\,m$ up to the radial station $r/R = 0.946$, followed by a parabolic tip with a reduction of chord length to $c = 0.046\,m$ at $r/R = 1.0$, leading to a rotor solidity of $\sigma = 0.085$. An airfoil of OA213-type was used up to $r/R = 0.75$ and OA209 above $r/R = 0.9$ with a transition of airfoil geometry in between. The blade features a $-8.3°$ linear twist and was meshed using a CH-topology for the aerodynamic part of the blade and a HH-like topology in the root and tip regions. The rotor shaft angle was set to the blind-test value

of 0° in this case and mesh sizes were 0.81 million for each blade and 2.85 million for the background grid. Simulations were carried out using both flow solvers FLOWer and TAU on identical meshes interpreting the structured FLOWer grid as unstructured for TAU and using a timestep corresponding to a 2° increment in rotor azimuth angle. For both flow solvers the RANS equations were closed employing the standard $k-\omega$ turbulence model according to Wilcox [18].

B. Trim Convergence

As stated above in section (II.C), a pure force trim was employed for this investigation.

Convergence of the control angles obtained from both solutions using TAU and FLOWer are presented in Fig. 1. The iterative trim process was stopped once the variations of all three control angles had fallen below 0.03°. The convergence speed of the iterative trim process is very similar using both toolchains and convergence was obtained after four re-trimming cycles.

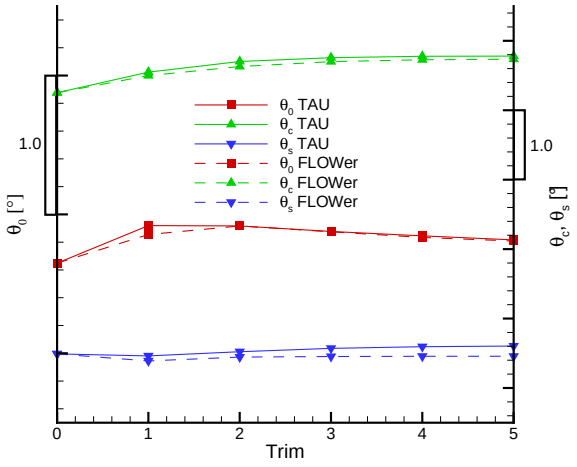

Figure 1: Convergence of control angles: comparison FLOWer–TAU

The corresponding evolution of the instationary rotor loads for the TAU computation is shown in Figure 2 where thick vertical lines mark the individual trim iterations. From this it can be seen that differences in the force distributions between successive trim iterations are significant during the first two or three cycles, whereas in the last two retrims (revolutions 8-12) no further changes are apparent. When comparing the control angles obtained in the FLOWer and TAU simulations, differences are damping out during convergence of θ_0 and θ_c and only the lateral angle θ_s finally produces a slight offset of 0.15°. In order to confirm that the prescribed trim objectives were met, instationary forces of the last quarter revolution of each trim cycle were averaged. This is shown in Figure 3. Trim objectives are displayed as straight lines without symbols, the TAU computation as solid and the FLOWer simulation as dashed lines. Subtle differences between the computed forces and the trim objectives are encountered using both toolchains.

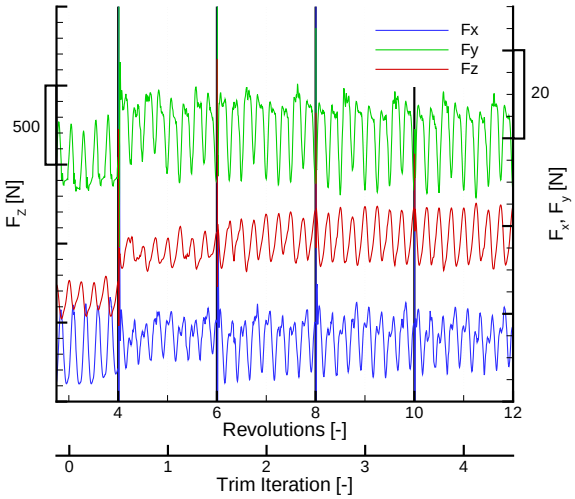

Figure 2: Development of (instationary) rotor loads over trim cycles / revolutions (TAU computation)

As already noted above, this flight case was expected to be difficult to converge during the trim iterations and the small deviations of the CFD-computed rotor loads from the trim objectives may be attributed to a not fully-converged solution within each trim step (only two rotor revolutions were computed per trim iteration).

C. Blade Dynamics

In Figures 4 and 5 the development of the blade dynamics is shown. The differences between the last two trim iterations are negligible for both motions, thus trim 3 and 4 are not shown here

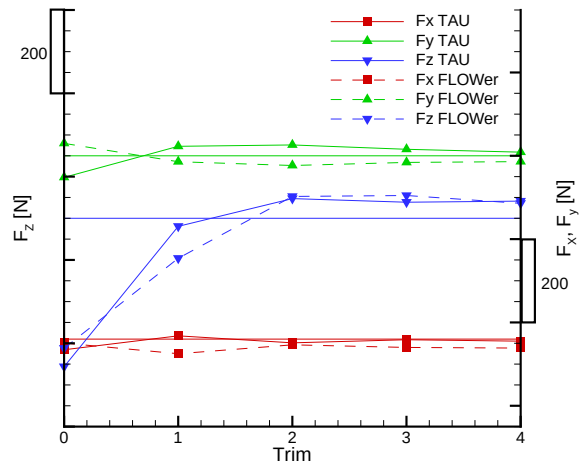

Figure 3: Convergence of average rotor loads: comparison FLOWer–TAU (last quarter revolution)

for clarity. The 4/rev-character of the tip torsion cannot be captured by the pure HOST calculation of trim 0 in contrast to the subsequent computations including corrections from three-dimensional CFD-data. While differences

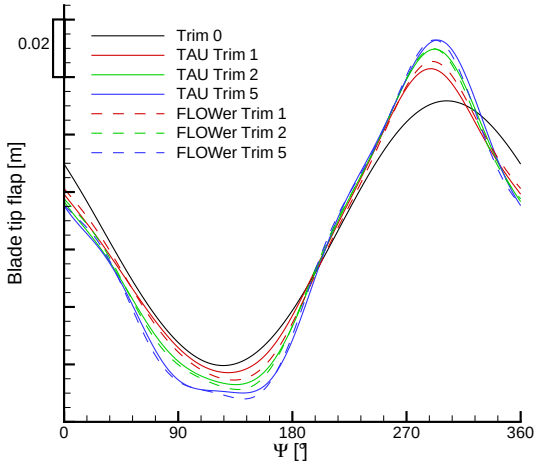

Figure 4: Development of blade tip flap: comparison FLOWer–TAU

between both toolchains in the flapping motion are insignificant, somewhat larger deviations are observed in blade tip torsion during the trim process. The greater differences that occur in the tip torsion are already suggested by the deviation in the lateral control angle of approximately 0.1° (see Figure 1).

D. Rotor Aerodynamics

Aerodynamics are first assessed by studying chordwise distributions of the inviscid forces. This is done by comparing the pressure coefficient at specified radii and azimuth angles for computations using FLOWer and TAU. In Figure 6, sample results from this analysis are shown for radial stations $r/R = 0.47$ and $r/R = 0.89$.

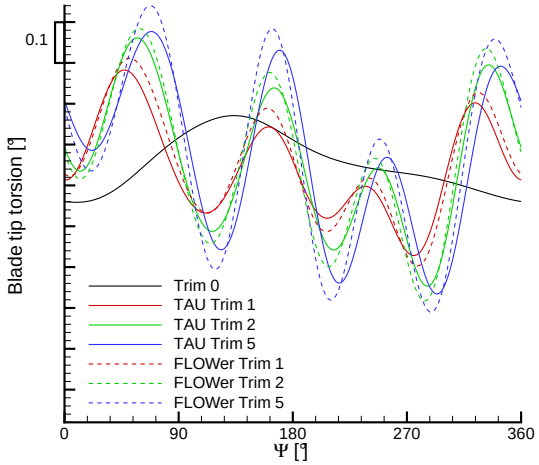

Figure 5: Development of blade tip torsion: comparison FLOWer–TAU

Both solutions appear to be in excellent agreement for the inner stations and only small differences occur on the outer radial position. TAU shows slight overpredictions of $c_{p,min}$ compared to FLOWer for most azimuthal positions. Only for $\Psi = 330°$ and $\Psi = 90°$ FLOWer shows a more pronounced leading-edge suction peak. Generally, good correlation between FLOWer and TAU has been achieved.

Azimuth- as well as radius-dependent distributions of the total vertical force on the rotor plane are plotted as contour plot in Figures 7 and 8. Contour levels are identical in both Figures. It can be seen that TAU predicts slightly higher loads on the retreating side in the range $\Psi = 210 \ldots 270°$ and on the advancing side around $\Psi = 110°$, an effect already suggested by the distributions of the pressure coefficients in Figure 6.

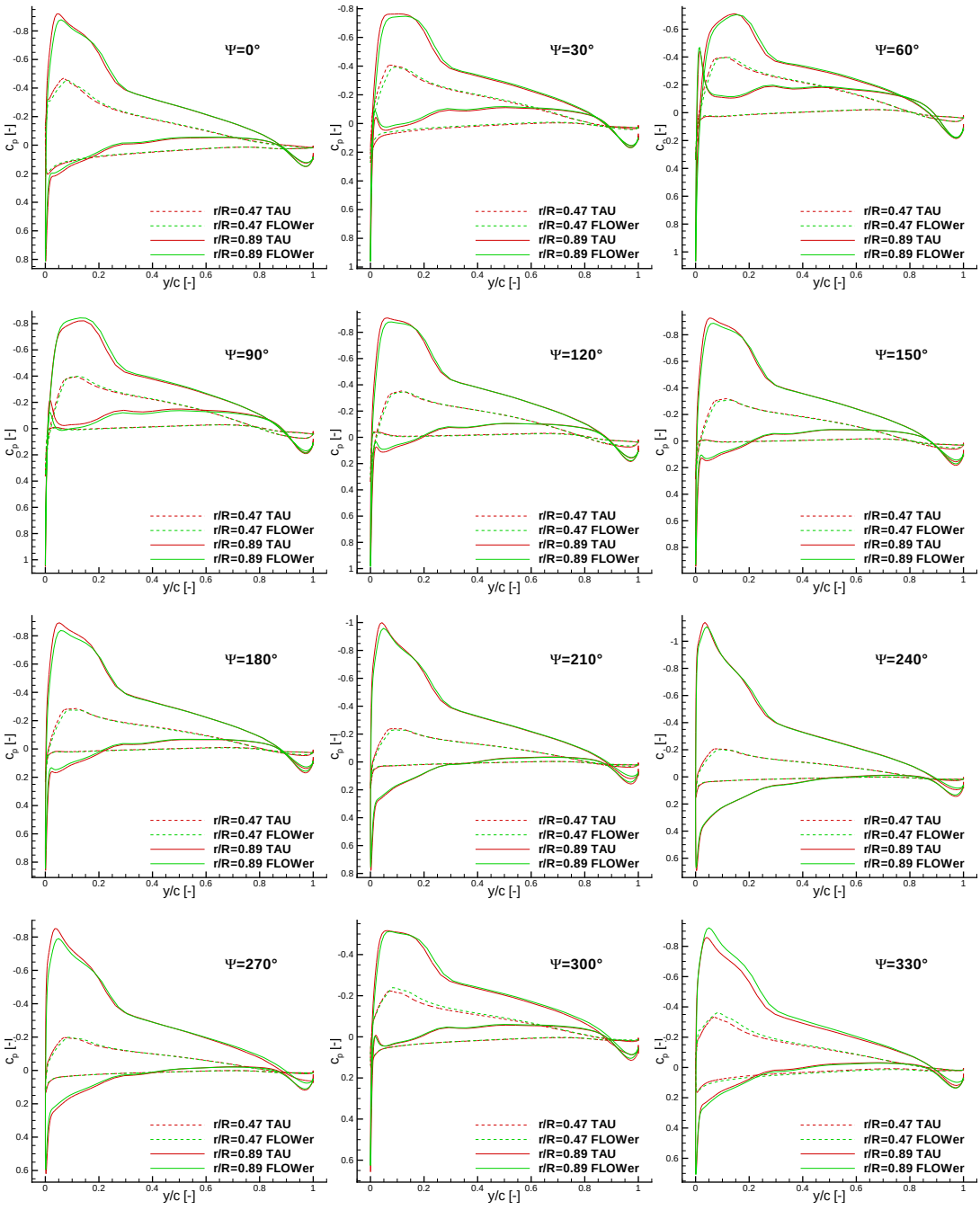

Figure 6: Chordwise c_p-distributions at two radial stations ($r/R = 0.47$ dashed, $r/R = 0.89$ solid) along azimuth angle: comparison FLOWer–TAU (Trim 4)

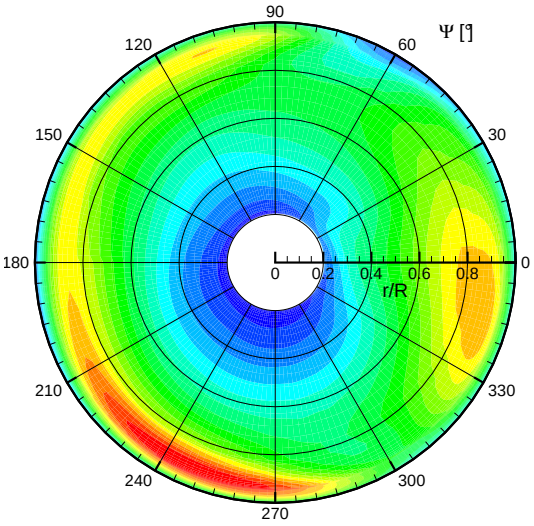

Figure 7: Distribution of the vertical force on the rotor plane F_z: TAU (Trim 4); Level differences $100\,N$

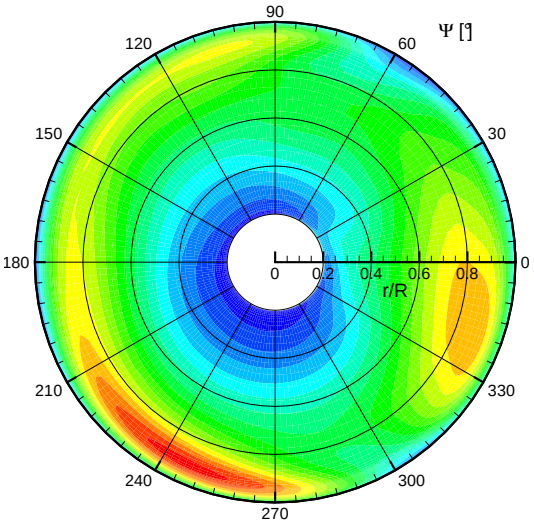

Figure 8: Distribution of the vertical force on the rotor plane F_z: FLOWer (Trim 4); Level differences $100\,N$

This may correspond to the lower magnitude of the θ_s control angle in Figure 1 in the TAU-computation since HOST tries to react to such higher loads by generating smaller amplitudes in blade torsion (Figure 5). The overall agreement between the two flow solutions however is good. For a more in-depth analysis, force coefficients corresponding to the sectional tangential (drag-directed) and normal (lift-directed) forces are plotted in Figures 9 and 10.

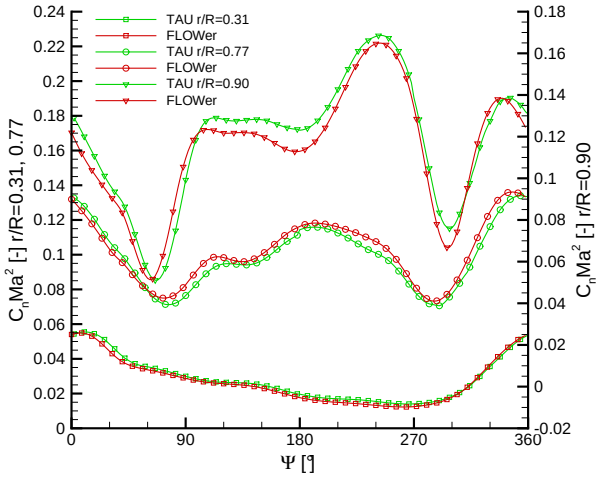

Figure 9: Azimuthal variation of the sectional normal force coefficient C_nMa^2 at radial stations $r/R = 0.31, 0.77$ and 0.90.

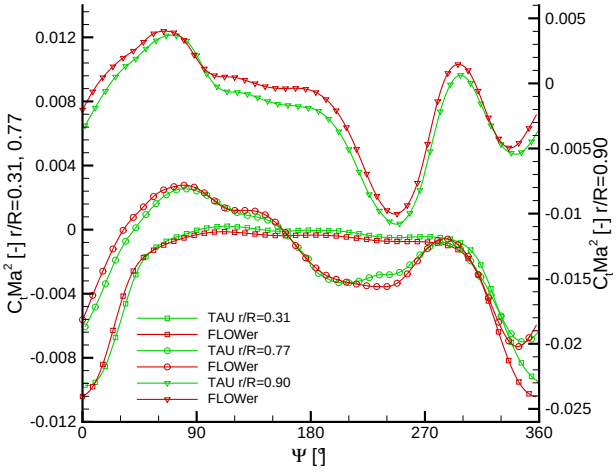

Figure 10: Azimuthal variation of the sectional tangential force coefficient C_tMa^2 at radial stations $r/R = 0.31, 0.77$ and 0.90.

Azimuthal variations of the Mach-normalized coefficients C_nMa^2 and C_tMa^2 are shown for radial stations $r/R = 0.31, 0.77$ and 0.90. Again, it can be observed that generally differences between the two codes are smaller at the inner sections of the blade. The maximum difference in the normal force coefficient at the outer radius

amounts to about 6 %. Trends are very similar.

In Figure 8, a vortex visualisation of the flow field is depicted using the λ_2 - criterion. Contour plots of λ_2 are shown for two distinct vertical slice planes and the pressure coefficient is plotted on the blade surfaces.

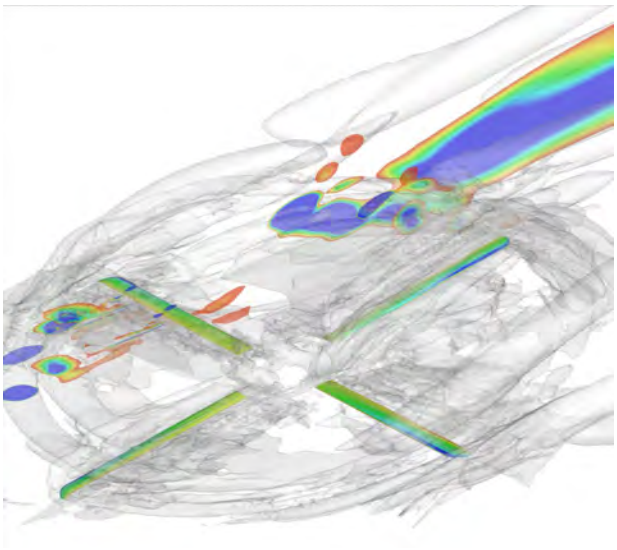

Figure 11: Vortex visualisation using the λ_2-criterion, blades: c_p-distribution (TAU-computation)

E. Computational Aspects

The setup used herein consists of about six million cells. As stated above, this simulation was performed using a weakly fluid-structure-coupled toolchain, i.e. computation of deformations, mesh deformation itself, solver preprocessing and flow solver had to be done each time step. Scalability was tested using this setup on 2^n $(n = 3, \ldots, 7)$ MPI processes and close to linear speed-up was measured for pure flux evaluation time as well as for the computational time needed for one entire coupling cycle as described above. Scaling performance strongly decreased above the maximum number of processes of 128 due to partition size. A recommendation of at least 10^5 cells per partition results in a maximum useful number of computational domains of about 60. In a test computation of 16 MPI-processes, performance was measured for the flux evaluation. Based on a clock rate of $2.8\,MHz$ of the local NEC Nehalem cluster's Intel Xeon X5560 processor, a performance of 8.5 GFLOPS (corresponding to 12% of a node's peak performance) was measured.

IV. Conclusions and Outlook

Problem areas in helicopter main rotor-fuselage interactional aerodynamics require a substantial increase in geometric complexity so that unstructured methods form an attractive alternative to current methods which are mostly based on structured approaches. In this work we presented the extension of a weak fluid-structure coupling interface to the computational environment of the unstructured TAU code. The new environment is based on a flexible Python-based implementation. Comparisons of our standard toolchain based on the structured solver FLOWer and the new implementation show good agreement in terms of trim convergence, blade dynamics and aerodynamic variables. The new toolchain shows good performance measures in both peak performance and in terms of scalability: for the current setup consisting of around six million cells, good scalability up to 128 MPI-processes and a maximum performance of 12% peak were observed. The aforementioned validation work on isolated rotors enables for progression to more elaborate configurations. Current investigations are steered towards the simulation of an entire helicopter similar to that of the GOAHEAD test campaign.

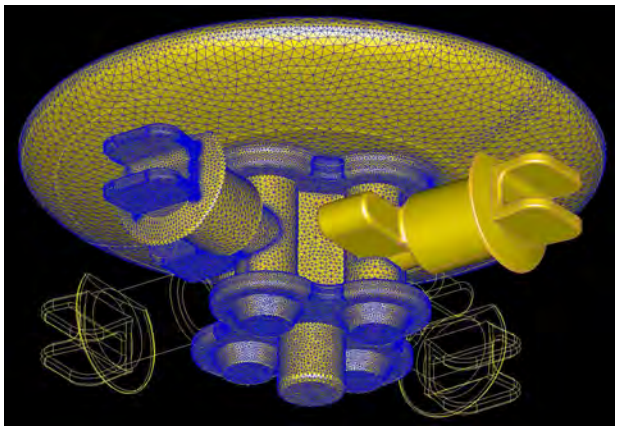

Figure 12: Detailed GOAHEAD CAD hub geometry and surface mesh

Figure 12 shows the CAD geometry and parts of a surface mesh of the detailed geometry of the rotor hub extracted from data of the GOAHEAD experiment. Figures 13 and 14 show the background mesh based on mixed element types (in this case prisms and tetraeders) for the entire fuselage and the vicinity of the hub region respectively. Particular attention will hereby be paid to the high speed tail shake case.

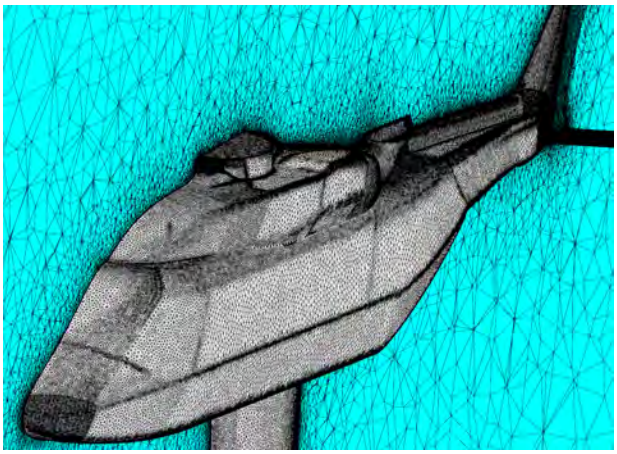

Figure 13: Mixed element background grid (GOAHEAD configuration)

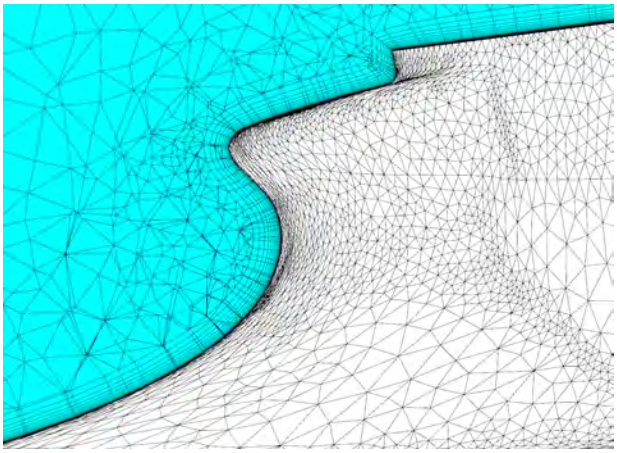

Figure 14: Close-up of the prismatic boundary layer grid hub region of the fuselage (GOAHEAD configuration)

Acknowledgements

This work has been supported by Deutsche Forschungsgemeinschaft (DFG) under grant KR 2959-1. We greatly acknowledge the provision of supercomputing time and technical support by the High Performance Computing Center Stuttgart (HLRS).

References

[1]Altmikus, A., Wagner, S., Beaumier, S., and Servera, G., "A Comparison: Weak versus Strong Modular Coupling for Trimmed Aeroelastic Rotor Simulations," *Proceedings of the 58th American Helicopter Society Annual Forum*, AHS, Montreal, Canada, 2004.

[2]Altmikus, A., *Nichtlineare Simulation der Strömungs-Struktur-Wechselwirkung am Hubschrauberrotor*, Ph.D. thesis, Institut für Aerodynamik und Gasdynamik, Universität Stuttgart, Germany, 2004.

[3]Altmikus, A. and Wagner, S., "On the Timewise Accuracy of Staggered Aeroelastic Simulations of Rotary Wings," *Proceedings of the AHS Aerodynamics, Acoustics and Test and Evaluations Technical Specialist Meeting*, AHS, San Francisco, CA, 2002.

[4]Dietz, M., Altmikus, A., Krämer, E., and Wagner, S., "Weak Coupling for Active Advanced Rotors," *Proceedings of the 31st European Rotorcraft Forum*, ERF, Florence, Italy, 2005.

[5]Dietz, M., *Simulation der Umströmung von Hubschrauberkonfigurationen unter Berücksichtigung von Strömungs-Struktur-Kopplung und Trimmung*, Ph.D. thesis, Institut für Aerodynamik und Gasdynamik, Universität Stuttgart, Germany, 2009.

[6]Khier, W., Dietz, M., Schwarz, T., and Wagner, S., "Trimmed CFD Simulation of a Complete Helicopter Configuration," *Proceedings of the 33rd European Rotorcraft Forum*, ERF, Kazan, Russia, 2007.

[7]Kampa, K., Enenkl, B., Polz, G., and Roth, G., "Aeromechanic Aspects in the Design of the EC135," *Proceedings of the 23rd European Rotorcraft Forum*, ERF, Dresden, Germany, 1997.

[8]Strehlow, H., Teves, D., and Polz, G., "Applied Helicopter Aeroelastics – Modelling and Testing," *Proceedings of the 22nd European Rotorcraft Forum*, ERF, Brighton, UK, 1996.

[9]Hassan, A., Thompson, T., Duque, E., and Melton, J., "Resolution of Tail Buffet Phenomena for AH-64D Longbow Apache^{TM}," *Proceedings of the 53rd American Helicopter Society Annual Forum*, AHS, Virginia Beach, VA, 1997.

[10]Benoit, B., Dequin, A.-M., Kampa, K., Grünhagen, W., Basset, P.-M., and Gimonet, B., "HOST, A General Helicopter Simulation Tool for Germany and France," *Proceedings of the 56th American Helicopter Society Annual Forum*, AHS, Virginia Beach, VA, 2000.

[11]Kroll, N., Eisfeld, B., and Bleeke, H., "FLOWer," *Notes on Numerical Fluid Mechanics*, Vol. 71, Vieweg, Braunschweig, 1999, pp. 58–68.

[12]Schwarz, T., *Ein blockstrukuriertes Verfahren zur Simulation der Umströmung komplexer Konfigurationen*, Ph.D. thesis, Institut für Aerodynamik und Strömungstechnik, Universität Braunschweig, Germany, 2005.

[13]Jameson, A., Schmidt, W., and Turkel, E., "Numerical Solutions of the Euler Equations by Finite Volume Methods using Runge-Kutta Time-Stepping Schemes," *Proceedings of the 14th AIAA Fluid and Plasma Dynamic Conference*, AIAA, Palo Alto, CA, 1981.

[14]Jameson, A., "Time dependent calculations using multigrid, with applications to unsteady flows past airfoils and wings," *Proceedings of the 10th Computational Fluid Dynamics Conference*, AIAA, Honolulu, HI, 1991.

[15]Guillard, H. and Farhat, C., "On the Significance of the GCL for Flow Computations on Moving Meshes," *Proceedings of the 37th AIAA Aerospace Sciences Meeting and Exhibit*, AIAA, Reno, NV, 1999.

[16]Yu, Y., Tung, C., van der Wall, B., Pausder, H., Burley, C., Beaumier, P., Delrieux, Y., Mercker, E., and Pengel, K., "The HART-II Test: Rotor Wakes and Aeroacoustics with Higher-Harmonic Pitch Control (HHC) Inputs – The Joint German/French/Dutch/US Project," *Proceedings of the 58th American Helicopter Society Annual Forum*, AHS, Montreal, Canada, 2002.

[17]Pahlke, K., "The GOAHEAD Project," *Proceedings of the 33rd European Rotorcraft Forum*, ERF, Kazan, Russia, 2007.

[18]Wilcox, D., *Turbulence Modeling for CFD, 2nd edition*, DCW Industries, Inc., La Cañada, CA, 1998.